Chapter 2 Literature Reviews

2-1 Structure, properties and nanofabrications of CNTs

2-1-1 Structures and properties of CNTs

For determine the structure of the CNT, scientists used the two spatial vectors to depict the feature of CNT as express in term as follows [Saito-92-2204]

$$\mathbf{C_h = na_1 + ma_2 \equiv (n,m)} \quad \textbf{(2-1)}$$

Where the C_h is chiral vector, a_1 and a_2 are the unit vectors of graphene sheet, where n and m are the integers. Figure 2-1 shows the chiral vector represent on the 2D graphene sheet, it indicates an included angle θ among C_h and a_1 called the chiral angle, that is respect to the zigzag axis at $\theta = 0^o$. The diameter (d) of CNT and the chiral angle θ can be express in term as follows

$$d = \frac{a\sqrt{m^2 + mn + n^2}}{\pi} \quad \textbf{(2-2)}$$

$$\theta = \sin^{-1}\left[-\frac{\sqrt{3}m}{2\sqrt{n^2 + nm + m^2}}\right] \quad \textbf{(2-3)}$$

The structures of CNTs in zigzag, armchair or chiral form are classified by the $\theta = 0^o$, $\theta = 30^o$, and $0^o < \theta < 30^o$, respectively. The chiral vector is expressed as a pair of integers (n, m) for mapping planar graphene sheet. The zigzag, armchair and chiral CNTs are corresponding to the chiral vectors of (n, 0), (n, n) and (n, m), respectively as shown in Fig. 2-2.

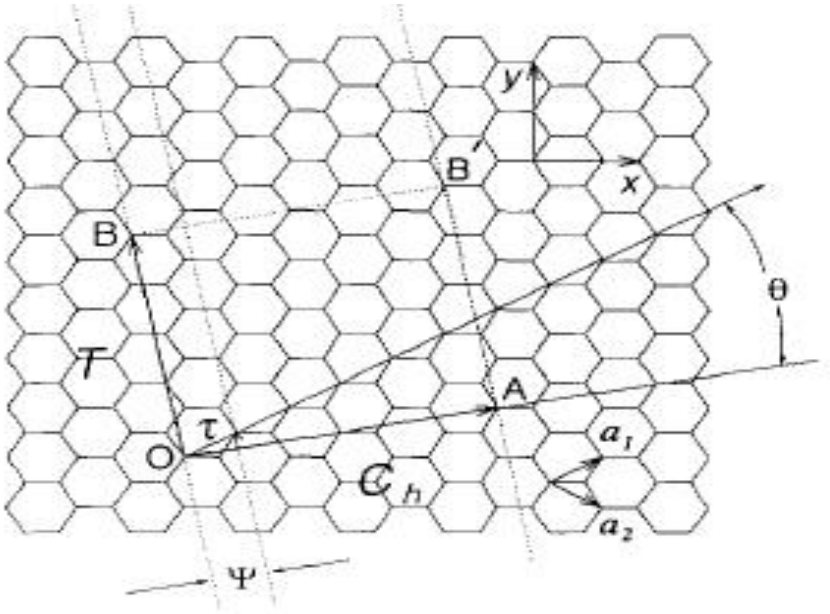

Fig. 2-1 Spatial vector representation on 2D graphene sheet [Dresselhaus -96-756].

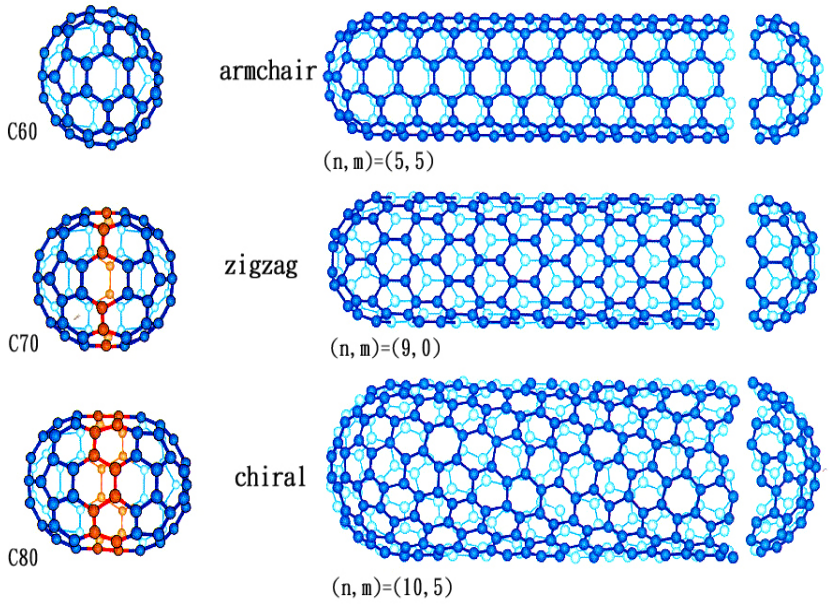

Fig. 2-2 CNT structures of armchair, chiral and zigzag tubules [Dresselhaus-96-756].

Theoretical [Hamada-92-1579; Saito-92-2204] and experimental calculations [Odom-1998-62] have predicted that all the electrical conductivity of armchair tubes are metallic, whereas, the zigzag and chiral tubes are either metallic or semiconducting which depending on its chirality as shown in Fig. 2-3. There have two possibilities of the chiral and zigzag nanotubes owning metallic or semiconducting conductivity: (a) If n-m = 3q, q ≠ 0, the CNT acts metallic conductivity with an energy gap of about 1.7-2.0 eV. (b) If n-m ≠ 3q, the CNT acts semiconducting conductivity with an energy gap of about 0.5-0.6 eV. These indicate the electrical properties of CNT are very sensitive to the chirality and the tube diameter.

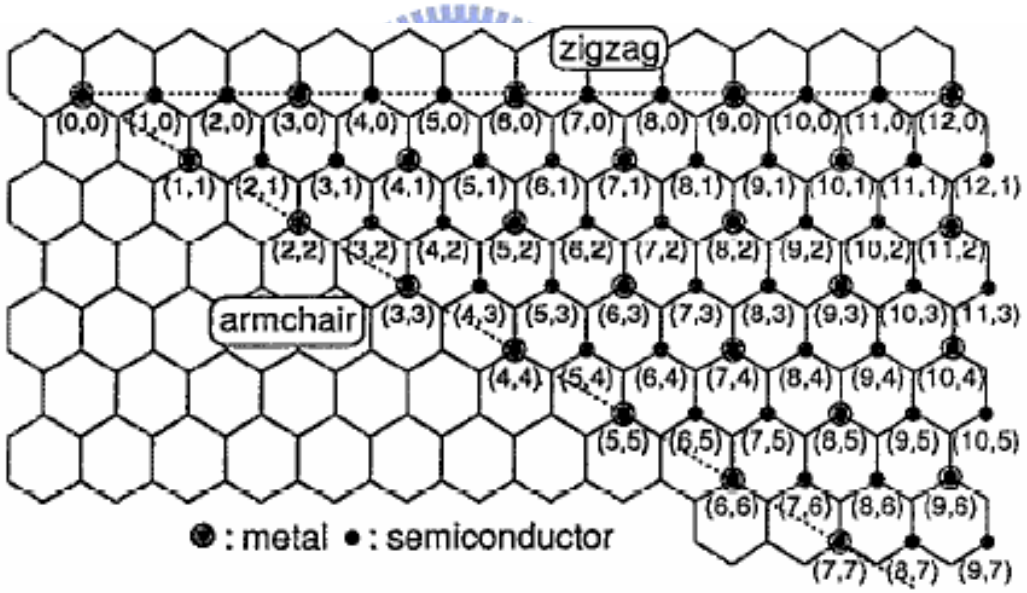

Fig. 2-3 The 2D graphene sheet is shown different electrical conductivity of zigzag, armchair and chiral nanotubes depending on its chirality [Saito-92-2204].

In electronically, metallic CNTs are expected to behave as ideal one-dimensional (1D) “quantum wires” which have ballistically electronic transport due to no scattering in the tube [Frank-98-1744]. Hence the CNT can carry high current with essentially no heating. In additional, an important and remarkable property is field emission (FE) properties. Due to the CNT with the small radius of tip comparing with its length thus enhance the FE properties. Table 2-1 are listed the threshold electric field of various material for field emitter at current density equal to 10 mA/cm^2. It indicates the CNTs owning extraordinary field emission comparing with other candidate for field emitters. The next section will review theory of field emission properties on CNT in detail. Further, The measured room temperature thermal conductivity for an individual MWNT (>3000 W/m*K) is grater than that of natural diamond and the basal plane of graphite (both ~ 2000 W/m*K) [Kim-01-215502].Superconductivity of SWCNT has also been observed, ~0.55 K for 1.4-nm-diameter SWNTs [Kociak-01-2416] and ~5 K for 0.5-nm-diameter SWNTs grown in zeolites [Tang-01-2462]. About the mechanical properties of nanotubes are fascinating. The CNTs are stronger than steel, light weight and having excellent flexibility. The strength of the carbon bonds makes CNT becoming one of the strongest and stiffest materials. On the basis of the in-plane elastic modulus of graphite, the axial elastic modulus of CNT is predicted to be at least 1000 GPa. The average Yong’s modulus of MWNT obtained ~1.8 TPa [Treacy-96-678]. It can be seen that MWNTs are the most superior mechanical characteristics. The hollow structure and closed topology of CNTs produce a distinct mechanical response in CNT compared to other graphite structure. The fracture and deformation modes of CNT are complex. CNTs can sustain extreme strains (40 %) in tension with out showing signs of brittle behavior, plastic deformation, or bond rupture. Table 2-2 shows the physical properties of CNTs with related materials [www.pa.msu.edu].

Table 2-1 The threshold electrical field for different materials at 10 mA/cm^2 current density. [Zhu-98-1471]

Material	Threshold electrical field (V/μm)
Mo tips	50-100
Si tips	50-100
p-type semiconducting dimond	130
Undoped, defective CVD diamond	30-120
Amorphous diamond	20-40
Cs-coated diamond	20-30
Graphite powder (<1 mm size)	17
Nanostructured diamond[a]	3-5 (unstable > 30 mA/cm^2)
Carbon nanotube[b]	1-3 (stable at 1 A/cm^2)

[a]Heat-treated in H plasma.

[b]random SWNT film.

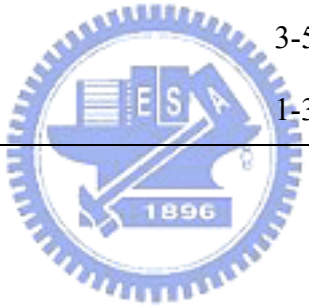

Table 2-2.The properties of graphite, diamond, C_{60} and carbon nanotube [http://www.pa.msu.edu]

Property	Graphite[a]	Diamond	C_{60}	Carbon nanotube
Lattice structure	Hexagonal	Cubic		
Space group	P63/mmc - D_{6h}^4	Fd3m - O_h^7		
Lattice constant (RT[b]) (Å)	2.462; 6.708	3.567	Fcc: 14.17	
Atomic density (C atoms/cm^3)	1.14 x 10^{23}	1.77 x 10^{23}		(10,10)armchair: 1.33 (17, 0) zigzag: 1.34 (12, 6) chrial: 16.52
Specific gravity (g/cm^3)	2.26	3.515	1.72	
Molecular density(/cm^3)			1.44 x 10^{21}	
Specific heat (cal/g • k)	0.17	0.12		
Thermal conductivity (RT) (W/cm-K)[c]	30; 0.06	~ 25	0.4	~ 2000
Binding energy (eV/C atom)	7.4	7.2		

Debye temperature (K)	2500	950	185	

Table 2-2 (Conti.)

Property	Graphite[a]	Diamond	C_{60}	Carbon nanotube
Bulk modulus (GPa)	286	422	6.8, 8.8	
Elastic moduli (GPa)	1060; 36.5	107.6		
Mohs hardness[e]	9; 0.5	10		
Young's module (GPa)	In plane:1000; C axis: 36	1000	15.9	~ 1000 (SWNT) ~ 1280 (MWNT)
Band gap (eV)	-0.04[d]	5.47		For (n, m); n-m is divisible by 3:0 For (n, m); n-m is not divisible by 3: ~ 0.5
Total carrier density (10^{18}/cm3 at 4K)	5	0		
Resistivity (Ωcm)	50 x 10^{-6}; 1	~ 1020		10-4
Dielectric constant (RT) (low frequency)	3.0; 5.0	5.58	4.0 – 4.5	
Melting point (K)	4450	4500	1180	
Thermal expansion coefficient (RT) (/K)	-1 x 10^{-6}; 29 x 10^{6}	~ 1 x 10^{-6}	6.6 x 10^{-5}	
Velocity of sound (cm/sec)	~ 2.63 x 10^{5}; ~ 1 x 10^{5}	~ 1.96 x 10^{5}	V_t: 2.1 x 10^{5}; V_l:3.6-4.31x10^{5}	
Highest first-order Raman frequency (cm^{-1})	1582	1332		

[a] For anostropic properties, the in-plane (*ab* plane or a-axis) value is given on the left and the c-axis value on the right.

[b] RT denotes room temperature (300 K)

[c] Highest reported thermal conductivity values are listed.

[d] A negative bandgap implies a band overlap, i.e., semimetallic behavior.

[e] A scale based on values from 0 to 10, where 10 is the hardest material (diamond) and 1 is talc.

2-1-2 Nanofabrication of CNTs

For synthesized the high yield and good quality CNTs, many method was invented and developed. Nowadays, several methods such as electric arc-discharge, laser ablation, vapor-condensation, thermal chemical vapor deposition (CVD), and plasma enhance CVD were employed to synthesize the CNTs. In all of these methods, carbon source formed can be solid, gas or polymer like. The usually used carbonaceous gas sources are including CH_4, C_2H_2, C_2H_4, CO and CO_2; Solid carbon source as like graphite target. Moreover precursor or buffer gases as H_2, Ar, N_2 and NH_3 were used to help the decomposition of carbon gas source gases and to keep the substrate activity. The CNTs can be synthesized with catalyst assisted or catalyst free, where the usually used catalyst as Fe, Co and Ni or their alloys. In follows will introduce mainly methods for synthesized CNTs.

(a) Arc-discharge method:

Arc-discharge method is also called arc vaporization method. It initially used for producing C_{60} fullerenes, is the most common and perhaps easiest way to produce CNTs as it is rather simple to undertake. However, it is a technique that produces a mixture of component and requires separating CNTs from the soots and the catalytic metals present in the crude product. For synthesize CNTs, two graphite rods placed end to end, the distance among two rods about 1 mm, in an enclosure that is usually filled with inert gas (He or Ar) at low pressure (50~700 mbar). A direct current of 50 to 100 A driven by ~20 V creates a high temperature discharge between the two electrodes. The discharge vaporizes one of the carbon rods and forms a small rod shaped deposit on the other rod. Producing CNTs in high yield depends on the uniformity of the plasma arc and the temperature of the deposit form on the carbon electrode [Ebbesen-92-220].

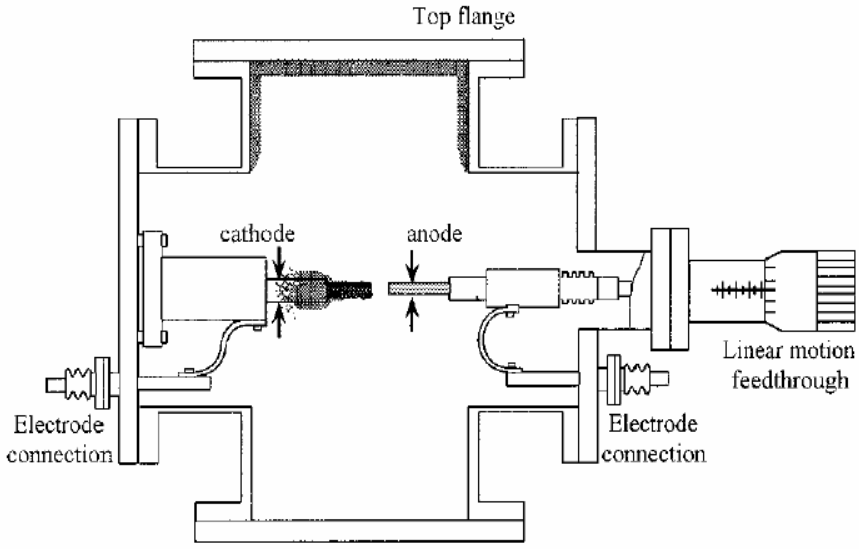

Fig. 2-4 Schematic drawing of arc-discharge system [Ebbesen-92-220].

(b) Laser ablation method:

The laser ablation was firstly reported by smalley's group at Rice University in 1995 [Guo-95-49]. The system of laser ablation method or called laser vaporization method is shown in Fig. 2-5. The CO_2 or YAG laser in continuous or pulse type, respectively, were employed to vaporize a target at 1200 ℃, where the target was consisted of graphite or graphite and metal composition. The oven is filled with the Ar or He gas in order to keep the pressure at 500 Torr. The vaporized species will deposit on the cooling copper finger or wire. If used catalyst assisted CNT growth can synthesized the SWNT in 1-nm-diameter. This merit of this method is that having higher yield than arc-discharge method, but the drawback is the as-grown CNTs need to purify in post-treatment.

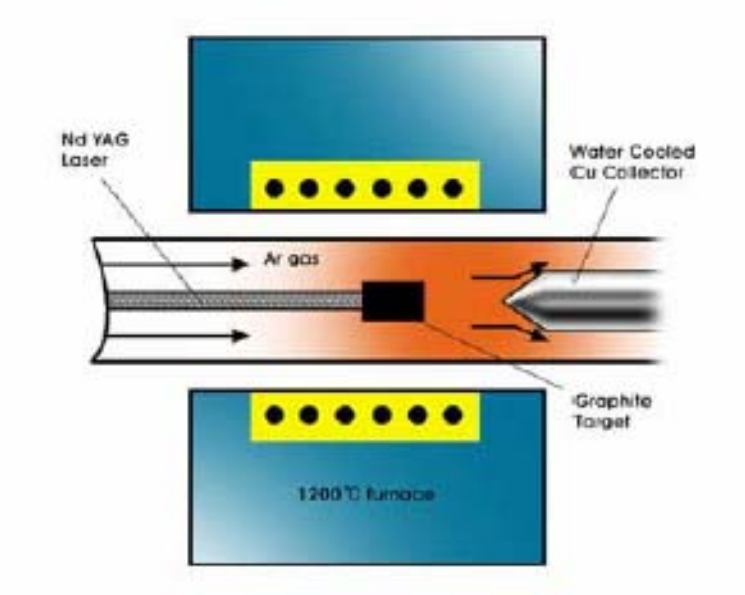

Fig. 2-5 Schematic drawings of a laser ablation apparatus [Guo-95-49].

(c) Thermal chemical vapor deposition:

Figure 2-6 shows a schematic diagram of thermal CVD apparatus in the synthesis of carbon nanotubes. The method was used pyrolysis of hydrocarbon source to synthesize the CNTs. This method is also catalyst assisted CNTs growth method and the quality of CNTs is sensitive to the pyrolysis temperature. The specimen is placed in a quartz boat with coated transition metals or theirs alloy on a substrate, and then the boat is positioned in a CVD reaction furnace, and nano-size fine catalytic metal particles are formed after an additional etching of the catalytic metal film with NH_3 gas at a temperature in 750 to 1050^{o}C. Reaction gas is supplied in one end of the apparatus, and gas outlet in the other [Lee- 01-245]. The merit of this method is easily to deposit large area, uniform and good quality of CNTs. However the drawback is not compatible with IC (integrated circuit) process due to working temperature over 600 ℃.

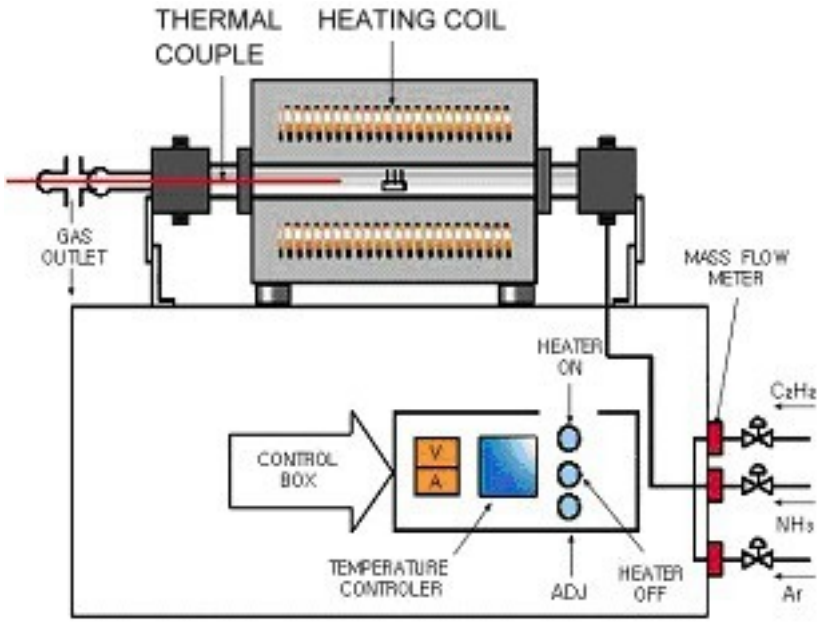

Fig. 2-6 Schematic drawings of thermal CVD system [Lee- 01-245]

(d) Methods of plasma chemical vapor deposition

Plasma CVD system was employed to deposit the CNTs with many merits comparing with other methods e.g. compatible process with IC process, cheaper, less contamination, high yielding and controlled alignment of CNTs, thus current attention has focused on developing new techniques for the preparation of vertically aligned CNTs by using CVD methods.

According to the methods of plasma excitation can be classified the different plasma system such as microwave plasma CVD (MPCVD), RF or DC bias excited plasma CVD (PECVD), microwave plasma assisted hot filament CVD (MP-HFCVD) and electron cyclotron resonance CVD (ECR-CVD) and so fourth. Generally, the power supplies for discharge of plasma CVD are DC bias; radio frequency (RF) (13.56 MHz) and microwave (2.47 GHz) are typical of high frequency power supply. Using the plasma CVD process to produce CNTs can be prepared by applying decomposition of hydrocarbon (such as CH_4, C_2H_2, C_2H_4 and C_6H_6) or monoxide and even decomposed of metal complex on various substrates that coated transition-metal film. The common used of microwave plasma CVD,

such as MP-CVD, PE-HF-CVD, and ECR-CVD, to synthesize CNTs can be ranked in terms of their working pressure, where MP-CVD or PE-HF-CVD and ECR-CVD were operated with the pressure range of $P < 10^{-3}$ Torr and $10^{-1} < P < 100$ Torr, respectively. The MP-CVD system [Qin-98-3437] as shown in Fig.2-7, with the high density of plasma ball permits a contamination-free and a modification of plasma shape through tuning of the cavity. The PE-HF-CVD system applied the current on the tungsten filament to efficiently increase temperature in the chamber [Kurt-01-1723] as shown in Fig. 2-8 The ECR-CVD as shown in Fig.2-9 is known for its own advantages of high dissociation percentage of the precursor gas, high uniformity of plasma energy distribution and large area of CNT deposition [Tsai-01-NCTU].

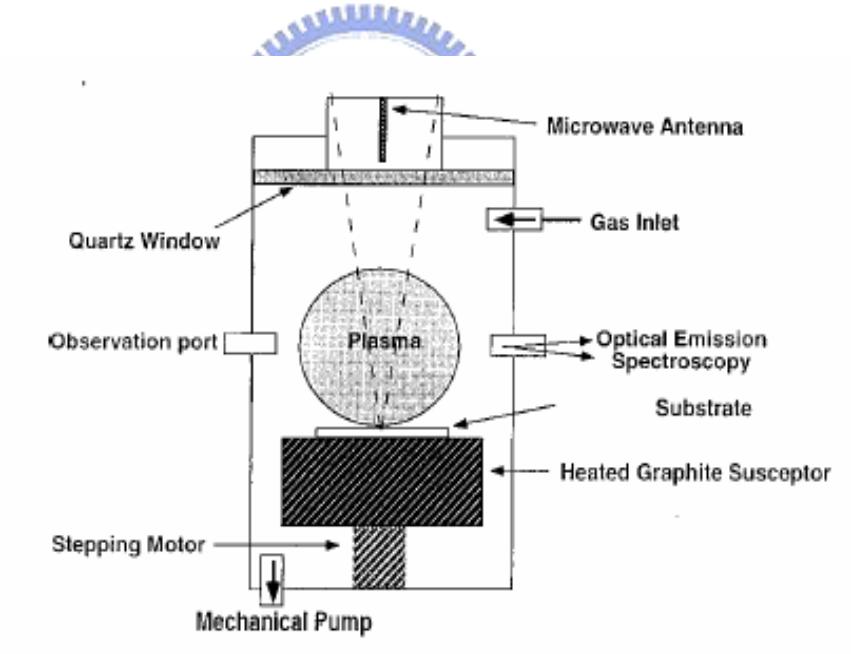

Fig. 2-7 Schematic drawing of MPCVD apparatus [Qin-98-3437].

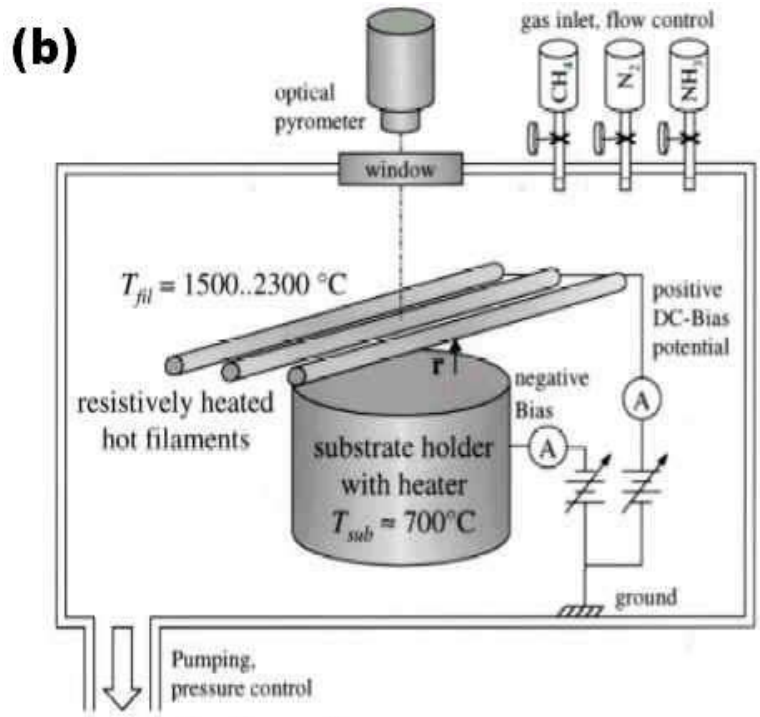

Fig. 2-8 Schematic drawing of PE-HF-CVD apparatus [Kurt-01-1723].

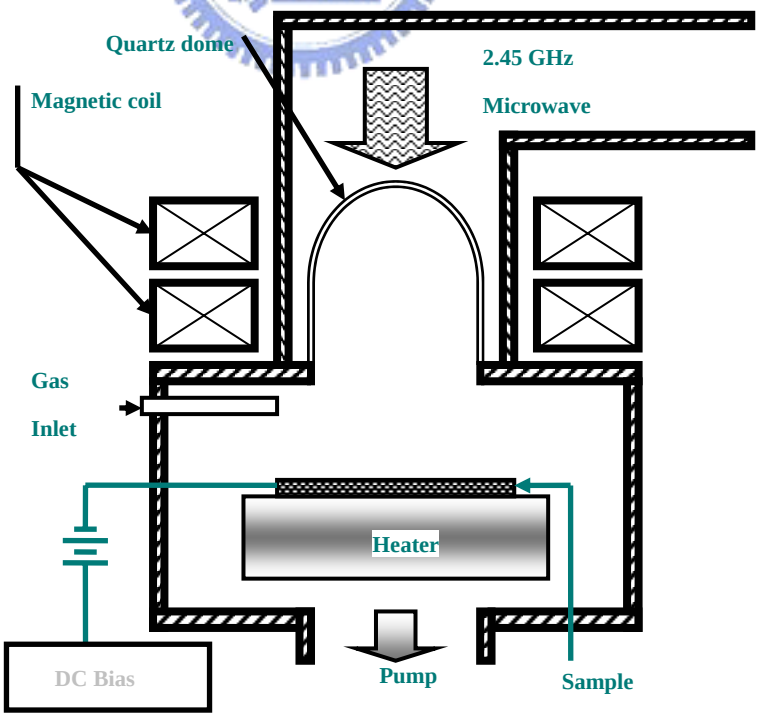

Fig. 2-9 Schematic drawing of MPCVD apparatus [Tsai-01-NCTU].

2-2 Applications of CNTs

2-2-1 Hydrogen storage

The advantage of hydrogen as energy source is that its combustion product is water. In addition, hydrogen can be easily regenerated. For this reason, a suitable hydrogen storage is necessary, satisfying a combination of both volume and weight limitation. The two commonly used means to store hydrogen are gas phase and electrochemical adsorption. Because of CNT has cylindrical and hollow geometry in nanoscale, it has been predicate that the carbon nanotubes can storage a liquid or gas in the inner cores through a capillary effect. As a threshold for economical storage, the Department of Energy (USA) has set storage requirement s of 6.5 % by weight as the minimum level for hydrogen fuel cells. Many reports are proposed that SWNTs were able to meet and sometimes exceed this level by using gas phase adsorption [Dollin-97-377; Ye-99-2307; Chen-99-91]. Yet, most experimental reports of high storage capacities are rather controversial so that it is difficult to assess the applications potential.

2-2-2 Lithium intercalation

The basic principle of rechargeable lithium batteries is electrochemical intercalation and de-intercalation of Li in both electrodes. An ideal battery has a high-energy capacity, fast charging time and long cycle time. The capacity is determined by the Li saturation concentration of the electrode material. The SWNTs have shown to possess both high reversible and irreversible capacities [Gao-99-153].

2-2-3 Electrochemical supercapacitors

Supercapacitors have a high capacitance and potentially applicable in electronic devices. Typically, they are comprised two electrodes separated by an insulating material that is ionically conducting in electrochemical devices. The capacity inversely depends on

the separation between the charges on the electrode and counter charge in the electrolyte. The CNTs has separation of electrodes in nanoscale so very large capacities result from the high CNT surface area accessible to the electrodes. In this way, a large amount of charge injection occurs if only a small voltage is supplied. This charge injection is used for energy storage in CNT supercapacitor [Niu-97-1480].

2-2-4 Field emitting devices

If a solid is subjected to a sufficiently high electric field, electrons near the Fermi level can be extra from the solid by tunneling trough the surface potential barrier. This emission current depends on the strength of the local electrical field at the emission surface and the work function. In order to extract electrons, the applied field must be very high. For technological applications, the emissive material should have a low threshold electric field, large stability at high current density, furthermore, ideal emitters required to have a nonoscale size diameter, a high electrical conductivity, a small energy spread and large chemical stability. The CNT possess all these properties, thus it is predicted becoming the best material for field emission device. For bottleneck in the use of CNTs on field emission is the conductivity and emission stability which depending on the fabrication process and synthesis conditions. Figure 2-10 show the 4.5 inch full-color CNT-field emission display that was fabricated by Samsung Corp. in Korea [Choi-99-3129]. It shows the brightness reaching 1800 cd/cm^2 at electrical field ~ 3.7 V/μm.

2-2-5 Transistors

The Field –Effect transistor can be constructed of only one semiconducting SWNT [Martel-98-2447]. By applying a voltage to a gate electrode, the CNT can be switched from a conducting to an insulating state. A schematic representation of such a transistor is given in Fig. 2-11. Such CNT transistors can be coupled tighter, working as a logical switch, which is the basic component of computers.

2-2-6 Nanoprobes and sensors

Because of their flexibility, nanotubes can be used in scanning probe instruments. Since MWNT-tips are conducting, they can be used in scanning tunneling microscopy (STM) [Orgass-01-281] and atomic force microscopy (AFM) [Dai-96-147] instrument. Advantages are the improved resolution in comparison as shown in Fig. 2-12 with conventional Si or metal tips and tips do not suffer from crashes with surfaces because of their high elasticity. The CNT tips can be modified chemically by attachment of functional groups. Because of this, CNTs can be used as molecular probes, with potential application in chemistry and biology. Other applications are as follows:

(a) A pair of nanotubes can be used as tweezers to move nanostructures on surface as shown in Fig. 2-13 [Kim-99-2148].

(b) Sheet of SWNTs can be used as electromechanical actuators, mimicking the actuator mechanism present in natural muscles [Baughman-99-1340].

(c) SWNTs may be used as miniaturized chemical sensors. On exposure to environments, with contain NO_2, NH_3, O_2, the electrical resistance changes [Kong-00-622].

2-2-7 Composite materials

The CNTs may be used as reinforcements in high strength, Low weight, and high performance composites due to their excellent mechanical properties. A main advantage of using CNTs for structural polymer composites is that CNT reinforcements will increase the toughness of the composites by absorbing energy during their highly flexible elastic behavior. Other advantages are the low density of the nanotubes, an increased electrical conduction and better performance during compressive load, or induced high thermal conductivity reinforced material.

Fig.2-10 Emitting image of fully sealed CNT-field emission display at color mode with red, green and blue phosphor columns [Choi-99-3129].

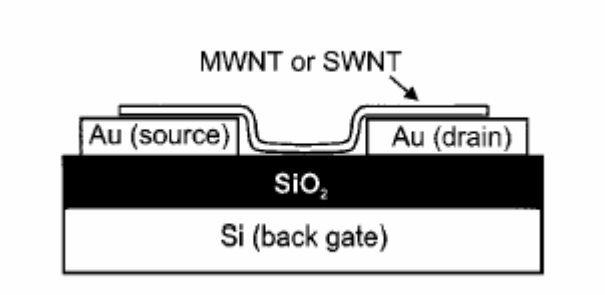

Fig. 2-11 Schematic cross section of the FET devices. A single SWNT or MWNT is bridges the gap between two gold electrodes. The Si substrate which is covered by a layer of SiO_2, acts as a back-gate [Martel-98-2447].

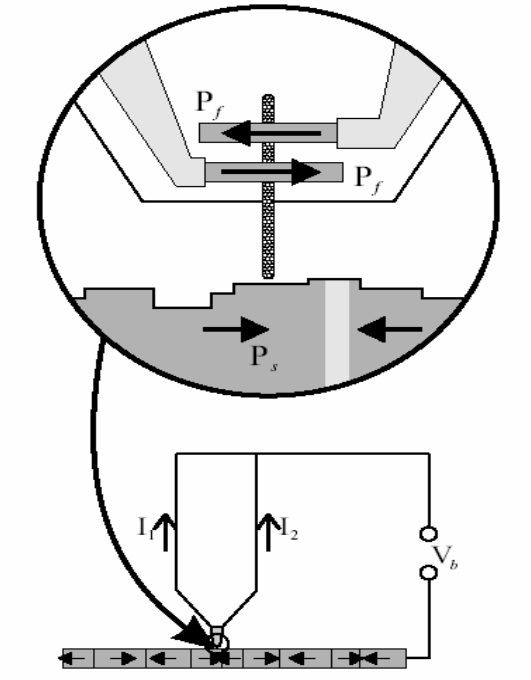

Fig.2-12 Schematic drawing of the spin-resolved CNT-STM. A CNT is acting tunneling tip in proximity to a magnetic sample with spin polarization P_s. The long mean-free path in the CNT is used to transport the tunnel current to two oppositely magnetized ferromagnetic electrodes. The spin polarization in the electrodes P_f causes an asymmetry between the currents through them (I_1 and I_2) [Orgass-01-281].

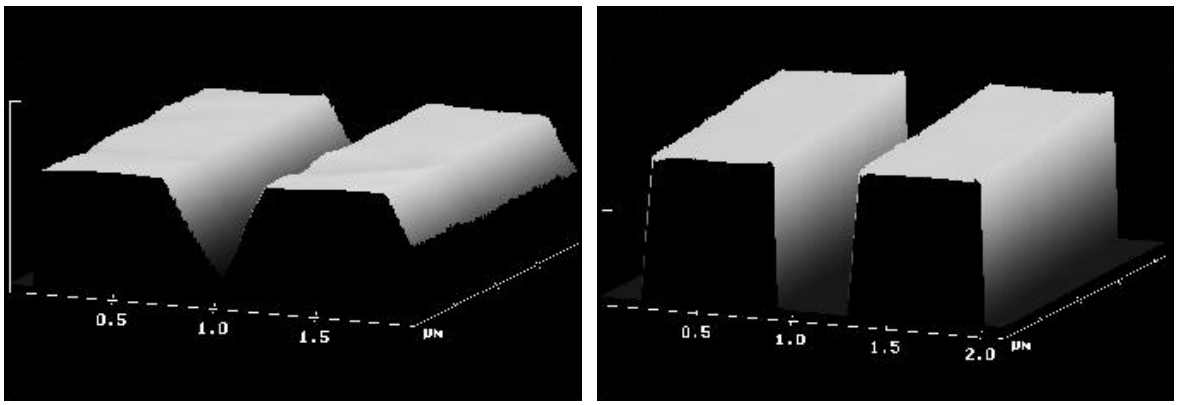

(a) (b)

Fig. 2-13 (a) Tapping mode AFM image scanning by conventional Si tip

(b) Tapping mode AFM image of CNTs tip scanning which provide better resolution than Si tip with the same specimen [Dai-96-147].

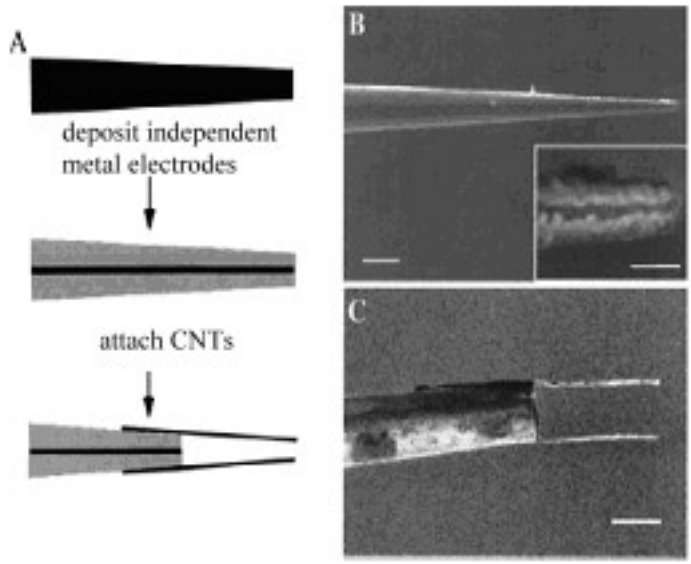

Fig. 2-14 Overview of the fabrication of CNT nanotweezers (A) schematic drawing the deposition of two independent metal electrodes and subsequent attachment of CNT and (B) SEM images are corresponding to the (A) , where the scale bar equal to 1 μm . The scale bar of inset HRSEM image is equal to 200 nm [Kim-99-2148].

2-3 Structure, properties and nanofabrication of CNCs

Many nanoscale conical carbon materials were discovered in last decade, Depending on the CNC structures can be divide into numerous type such as amorphous carbon nanocone [Jang-01-1682; Tsai-02-1821; Huang-03-6796], diamond nanocone [Jan-99-772], diamond-like carbon nanocone [Lin-01-126], cone-like carbon nanofiber [Merkulov-01-1178], tubular graphite CNC [Zhang-03-472; Hayashi-04-2886], as-grown amorphous coated Si tips [Bai-03-185], amorphous carbon nitride tips [Liu-00-304], SiC-capped nanotips [Lo-03-1420], and self-embedded nanocrystalline chromium carbides on polycrystalline CNCs [Tasi-03-4337]. The nanoscale conical carbon materials with infrastructure can explain with the basis of fullerene are proposed by Ge and Sattler [Endo-96-5]. STM measurement show that nanocones, made by deposition of very hot carbon on highly oriented pyrolitic graphite (HOPG) surface [Sattler-95-915]. It often tends to have an opening angle of ~20^0. Such caps may be of five possible opening angles (e.g., from 112.9^0 to 19.2^0) depending on the number of pentagonal disclinations clustered at the tip of cone as shown in Fig. 2-15. The function of the number of pentagons and angle of the cone can express as follow:

$$\theta' = 180 - (360/\pi)\cos^{-1}[1-(n/6)] \qquad (2\text{-}4)$$

where the θ' is the angle of the cone n means the number of the pentagons.

It has few literatures reported about the physical and chemical properties of CNC. However, the CNC can be considered an allotrope of carbon which consisted of the graphene layers and amorphous carbon, thus the basic properties may resemble the CNT. Due to CNC is carbon-based material and presented small radius with ultra sharp apex angle thus it was predicted having excellent FE properties. Many reports indicate the CNCs having the lower turn on electric field electric about 0.1~ 1.38 V/μm [Jang-01-1682;; Lo-03-1420; Tasi-03-4337; Huang-03-6796] and larger field enhancement factor β than film-type CNTs. Further, the cone-shape structure provides higher mechanical and thermal stability than a narrow

cylinder [Merkulov-01-1178]. Hence, the CNCs have potential not only as FE device but as a rigid tip for scanning probe microscopy.

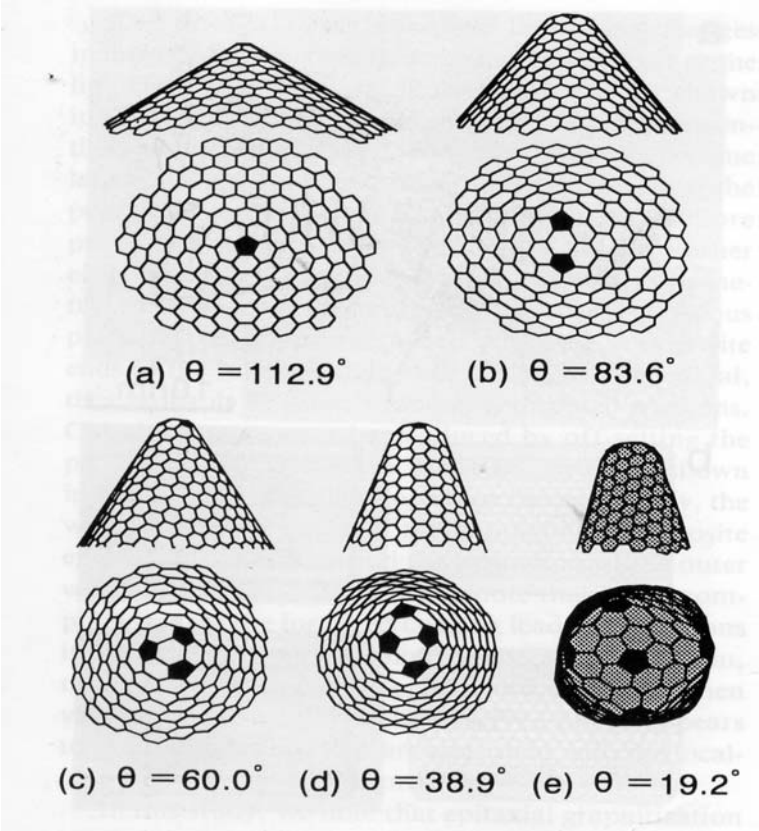

Fig.2-15 The possible tip structure with cone shape, in which the pentagons are included.

According to the literatures, the process conditions for synthesize the numerous CNCs are arranged in the Table 2-2. The nanofabrication methods of CNCs are similar to the CNTs as described above in section 2-1-2. By comparing the process parameter in Table 2-2, it can observe the CNCs prefer grown under bias applied conditions with or without catalyst assisted growth, but the ratio of precursor gas is extremely different. It is interesting to note that some case of grown CNCs only under low substrate temperature (~200 ℃), it implies the CNCs compatible with IC fabrication at low temperature process, comparing with typical process temperature of grown CNTs should maintain at above 600 ℃

Table 2-3 Summaries of synthetic methods of CNCs in the literatures

Synthesis system	**Substrate**	**Applied bias (V)**	**Pretreatment**	**Mixed gases (sccm)**	**Growth temp. (℃)**	**Cone structures**	**Ref.**
MPCVD	Si	-100~ -180		CH_4+H_2 (1~7.5 vol.%) + 100 vol.%	650	DLC	[Jan-99-772]
MPCVD	Si		H_2 100sccm; 20 min; 400W	CH_4+H_2 (6+294)	500 ~ 700	DLC	[Lin-01-126]
PEHFVD	Si	-600		CH_4+N_2+H_2 (3~10+20+60)	850	Si tips coated a-C	[Bai-03-185]
MPCVD	Si	<-130		CH_4+CO_2 (30+30)		Tip a-C; Lateral microcrystalline Graphite	[Tasi-02-1821]
ECRCVD	Si	-400		C_2H_2+N_2+Ar (100+300+10)	100~ 150	a-C:N	[Liu-00-304]
HDPCVD	Ni 70Å	No	NH_3 plasma	C_2H_2+H_2 (25/50)	700	$NiSi_2$ formation a-c film deposited then grapheme sheets	[Lim-02-864] [Jang-01-1682]

Table 2-3 (Conti.1)

Synthesis system	Substrate	Applied bias (V)	Pretreatment	Mixed gases (sccm)	Growth temp. (℃)	Cone structures	Ref.
PECVD	Ni-Fe/Ti Ni/Ti (10/10) nm dots	510~575 100 mA	NH_3 plasma 700℃	C_2H_2+NH_3 (40~60+80)	700	Central cylindrical CNF Sloped outer walls (tip-growth)	[Merkulov-01-1178] [Merkulov-01-381]
PECVD	Ni/W-Ti (10/10) nm film Ni/Ti (10/10) nm dots	555~575 100 mA	NH_3 plasma 700℃	C_2H_2/NH_3 (0.59) ratio He	700	Central cylindrical CNF Sloped outer walls (tip-growth)	[Merkulov-02-496]
MPCVD	Iron needle	-150		CH_4+N_2 (3+200)	~870	Coaxial tubular Graphite sheets (based-growth)	[Zhang-03-472]
MPCVD	Ni/SiO_2/Si	-450	H_2 plasma		350~750	(based-growth)	[Hayashi-04-2886]

Table 2-3 (Conti.2)

Synthesis system	**Substrate**	**Applied bias (V)**	**Pretreatment**	**Mixed gases (sccm)**	**Growth temp. (℃)**	**Cone structures**	**Ref.**
MPCVD	Oblique-cut Si (111)	-250		CH_4+H_2 2~30 vol.% + 100 vol.%		DLC and SiC	[Yeh-01-3609]
MPCVD	Cu	-50 ~ -250		CH_4+H_2 (14+47)	200	Amorphous carbon	[Huang-03-6979]
ECRCVD	Si (111)			CH_4+H_2+ Ar+SiH_4 1+8+5+0.2	200	SiC capped Si tips	[Lo-03-1420]
MPCVD	Cr/SiO_2/Si		H_2 plasma	CH_4+H_2 (10+25)	800	Nanocrystalline Cr embedded in CNCs	[Tasi-03-4337]